GROTH, P. & HAMMER, H. (1968). *Acta Chem. Scand.* **22**, 2059–2070.
International Tables for X-ray Crystallography (1974). Vol. IV. Birmingham: Kynoch Press. (Present distributor Kluwer Academic Publishers, Dordrecht.)
KAYE, A., NEIDLE, S. & REESE, C. B. (1988*a*). *Tetrahedron Lett.* **29**, 1841–1844.
KAYE, A., NEIDLE, S. & REESE, C. B. (1988*b*). *Tetrahedron Lett.* **29**, 2711–2714.
KAYE, A. & REESE, C. B. (1989). Unpublished data.
MAIN, P., FISKE, S. J., HULL, S. E., LESSINGER, L., GERMAIN, G., DECLERCQ, J.-P. & WOOLFSON, M. M. (1982). *MULTAN82. A System of Computer Programs for the Automatic Solution of Crystal Structures from X-ray Diffraction Data.* Univs. of York, England, and Louvain, Belgium.
MITSUYA, H. & BRODER, S. (1986). *Proc. Natl Acad. Sci. USA*, **83**, 1511–1516.
OLSON, W. K. & SUSSMAN, J. L. (1982). *J. Am. Chem. Soc.* **104** (1), 270–278.
POST, M. L., HUBER, C. P., BIRNBAUM, G. I. & SHUGAR, D. (1981). *Can. J. Chem.* **59**, 238–245.
RAAP, J., VAN BOOM, J. H., VAN LIESHOUT, H. C. & HAASNOOT, A. G. (1988). *J. Am. Chem. Soc.* **110**, 2736–2743.
ROHRER, D. C. & SUNDARALINGAM, M. (1970). *J. Am. Chem. Soc.* **92** (16), 4950–4955.
SAENGER, W. (1983). *Principals of Nucleic Acid Structure.* Berlin: Springer-Verlag.
SERIANNI, A. S. & CHIPMAN, D. M. (1987). *J. Am. Chem. Soc.* **109** (18), 5297–5303.
SUHADOLNIK, R. J. (1979). *Nucleosides as Biological Probes.* New York: John Wiley.
TSUKUDA, BY. & KOYAMA, H. (1970). *J. Chem. Soc. B*, pp. 1709–1712.
WALKER, N. & STUART, D. (1983). *Acta Cryst.* A**39**, 158–166.

Acta Cryst. (1990). B**46**, 431–440

Crystal Structures and Solid-State Photochemistry of Dimorphic Dibenzobarrelenes: Enantioselectivity of the Di-π-methane Rearrangement in the Solid State

BY MIGUEL GARCIA-GARIBAY, JOHN R. SCHEFFER, JAMES TROTTER AND FRED C. WIREKO

Department of Chemistry, University of British Columbia, Vancouver, BC, Canada V6T 1Y6

(*Received* 6 *July* 1989; *accepted* 15 *January* 1990)

Abstract

The diisopropyl diester derivative of dibenzobarrelene is dimorphic; one of the dimorphs crystallizes in a chiral space group ($P2_12_12_1$), while the other crystallizes in an achiral space group (*Pbca*). The chiral crystal undergoes a stereospecific photorearrangement to yield the corresponding dibenzosemibullvalene in near-quantitative enantiomeric excess, and the absolute configurations of the starting material and the product have been determined (with reasonable, although not complete certainty). Steric arguments, coupled with the absolute configurational relationship between the starting material and its photoproduct, have been used to rationalize the enantioselective pathway of the rearrangement in the solid state. Crystal data are: $T = 295$ K, Mo $K\alpha_1$, $\lambda = 0{\cdot}70930$ Å, or Cu $K\alpha_1$, $\lambda = 1{\cdot}54056$ Å; diisopropyl 9,10-dihydro-9,10-ethenoanthracene-11,12-dicarboxylate (form *a*, ^{i}Pr/^{i}Pr-*a*), $C_{24}H_{24}O_4$, $M_r = 376{\cdot}45$, orthorhombic, $P2_12_12_1$, $a = 8{\cdot}3488$ (9), $b = 11{\cdot}7036$ (9), $c = 21{\cdot}8060$ (13) Å, $V = 2130{\cdot}7$ (3) Å^3, $Z = 4$, $D_x = 1{\cdot}173$ g cm^{-3}, μ(Cu) = 6·0 cm^{-1}, $F(000) = 800$, $R = 0{\cdot}069$ for 3101 observed reflections; diisopropyl 9,10-dihydro-9,10-ethenoanthracene-11,12-dicarboxylate (form *b*, ^{i}Pr/^{i}Pr-*b*), $C_{24}H_{24}O_4$, $M_r = 376{\cdot}45$, orthorhombic, *Pbca*, $a = 9{\cdot}738$ (2), $b = 17{\cdot}092$ (3), $c = 25{\cdot}080$ (5) Å, $V = 4174$ (1) Å^3, $Z = 8$, $D_x = 1{\cdot}198$ g cm^{-3}, μ(Mo) = 0·75 cm^{-1}, $F(000) = 1600$, $R = 0{\cdot}044$ for 1299 observed reflections; diisopropyl 4b,8b,8c,8d-tetrahydrodibenzo[*a,f*]cyclopropa[*cd*]pentalene-8c,8d-dicarboxylate (^{i}Pr/^{i}Pr-*ap*), $C_{24}H_{24}O_4$, $M_r = 376{\cdot}45$, tetragonal, $P4_32_12$, $a = 10{\cdot}1889$ (2), $c = 38{\cdot}6347$ (5) Å, $V = 4010{\cdot}8$ (1) Å^3, $Z = 8$, $D_x = 1{\cdot}247$ g cm^{-3}, μ(Cu) = 6·4 cm^{-1}, $F(000) = 1600$, $R = 0{\cdot}036$ for 2879 observed reflections. The molecular structures of the dimorphs are similar to each other, except in the region of the α,β-unsaturated carbonyl system where the extents of conjugation of the ester groups to the central double bond are different in the two dimorphs. The ring skeletons of the dibenzobarrelenes and the dibenzosemibullvalene are similar to the corresponding units of the unsymmetrical 11,12-diester derivatives in previous work. The enantioselective pathway leading to the formation of ^{i}Pr/^{i}Pr-*ap* is consistent with steric packing effects, estimated from qualitative visual inspection of the packing environment around the ester groups, and from van der Waals intermolecular steric energy changes resulting from the movement of the ester groups.

Introduction

Previous crystal structure studies of 11,12-diester derivatives of dibenzobarrelene with non-equivalent ester groups ($E' \neq E$, Fig. 1) (Garcia-Garibay,

0108-7681/90/030431-10$03.00

Scheffer, Trotter & Wireko, 1990; Garcia-Garibay, 1988; Scheffer, Trotter, Garcia-Garibay & Wireko, 1988) have given detailed information on the structural aspects of the regioselective pathways in the solid-state photochemistry of this class of compound. These reactions proceed *via* the di-π-methane rearrangement (Zimmerman, 1980; Hixson, Mariano & Zimmerman, 1973; Zimmerman, Keck & Pflederer, 1976) to give, in general, two photoproducts (2) and (2′), which are regioisomerically related (Fig. 1), together with their enantiomorphs. The pathways leading to the formation of the major products in the solid state have been examined from electronic and steric points of view; correlation of structural and photochemical data has shown that the favoured pathways are explicable in terms of steric packing factors (Garcia-Garibay *et al.*, 1990).

In the present paper we report that the diisopropyl diester derivative of dibenzobarrelene ($E' = E = CO_2{}^i$Pr) is dimorphic. The molecule is achiral, but the dimorph designated ^{i}Pr/^{i}Pr-*a* crystallizes in a chiral space group ($P2_12_12_1$). Photolysis of the crystals of ^{i}Pr/^{i}Pr-*a* shows the production of ^{i}Pr/^{i}Pr-*ap* in quantitative enantiomeric excess (Evans, Garcia-Garibay, Omkaram, Scheffer, Trotter & Wireko, 1986); similar treatment of the other dimorph, designated ^{i}Pr/^{i}Pr-*b* (achiral space group *Pbca*), gives no optically active photoproducts. The electronic and steric arguments that were employed in an attempt to explain the regioselectivity in the solid state of the unsymmetrical 11,12-diester derivatives (Garcia-Garibay *et al.*, 1990) are invoked in order to rationalize the observed enantioselectivity of the photochemical rearrangement of ^{i}Pr/^{i}Pr-*a* in the solid state.

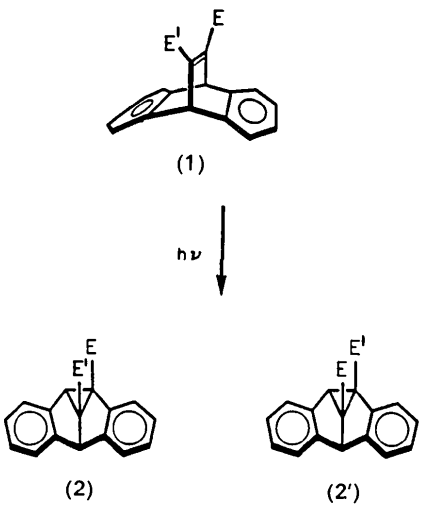

Fig. 1. Di-π-methane rearrangement in dibenzobarrelenes ($E = CO_2R$).

Experimental

It was observed during preliminary X-ray crystallographic investigation of the crystals of the diisopropyl diester derivative of dibenzobarrelene grown from cyclohexane that crystals from the same batch gave two different sets of cell parameters. It was, however, not possible to differentiate one crystal form from the other based on crystal morphology (prism). Crystals of the same compound obtained from ethanol gave only one of the dimorphs, designated ^{i}Pr/^{i}Pr-*b*. The other crystal modification found upon crystallization from cyclohexane (also the only dimorph observed on crystallization from the melt) is designated ^{i}Pr/^{i}Pr-*a*. The absolute configurations of ^{i}Pr/^{i}Pr-*a* and its solid-state photoproduct, ^{i}Pr/^{i}Pr-*ap*, have been determined by X-ray anomalous-dispersion techniques. To ensure that the absolute configuration of the product can be correlated with that of the starting material, a large single crystal of ^{i}Pr/^{i}Pr-*a* was grown. A small cut fragment of this crystal was used for data collection and structure determination of ^{i}Pr/^{i}Pr-*a*. Photolysis of the remaining large crystal resulted in ^{i}Pr/^{i}Pr-*ap*.

The general procedures and parameters of data collection are summarized in Table 1. Intensities were measured at 295 K with a CAD-4F diffractometer, ω–2θ scan (extended 25% on each side for background measurement), horizontal aperture (2·0 + tanθ) mm, vertical aperture 4 mm; three standard reflections measured periodically (no significant intensity variation). Mo $K\alpha$ (graphite monochromator) or Cu $K\alpha$ (nickel-filtered) radiations were used (Table 1). Two sets of data were collected for ^{i}Pr/^{i}Pr-*a* ($hk\bar{l}$ and $\bar{h}k\bar{l}$) and for ^{i}Pr/^{i}Pr-*ap* (hkl, $k \geq h$ and hkl, $h \geq k$); the two sets of reflections in each case are expected to have slightly different intensities in the presence of anomalous-dispersion effects. Absorption errors are negligible and no corrections were applied. Reflections with $I \geq 3\sigma(I)$ were considered observed, where $\sigma^2(I) = S + 4(B_1 + B_2) + (0{\cdot}04S)^2$, with S = scan, B_1 and B_2 background counts. All three structures were determined by direct methods with the use of *MULTAN*80,* using the $hk\bar{l}$ data for ^{i}Pr/^{i}Pr-*a*, and hkl, $k \geq h$ data for ^{i}Pr/^{i}Pr-*ap*. Refinement was by full-matrix least-squares methods on F, minimizing $\sum w(|F_o| - k|F_c|)^2$, with $w = 1/\sigma^2(F)$ giving uniform values of $\sum w\Delta F^2$. High apparent thermal motion of the terminal methyl C atoms in ^{i}Pr/^{i}Pr-*a* indicated some disorder which was resolved after the two sets of data were combined. The disorder was treated by distributing each of the four methyl C atoms involved

* Programs used include locally written programs and locally modified versions of *MULTAN*80 (Main, Fiske, Hull, Lessinger, Germain, Declercq & Woolfson, 1980); *ORFLS* and *ORFFE* (Busing, Martin & Levy, 1962, 1964), and *ORTEP*II (Johnson, 1976).

Table 1. *Data-collection and refinement parameters for dibenzobarrelenes and dibenzosemibullvalene*

	^{i}Pr/^{i}Pr-*a*	^{i}Pr/^{i}Pr-*b*	^{i}Pr/^{i}Pr-*ap*
Solvent	Cyclohexane	Ethanol	Ethanol
Dimensions (cut fragments) (mm)	0·3 × 0·25 × 0·2	0·35 × 0·3 × 0·3	0·35 × 0·35 × 0·3
Radiation	Cu $K\alpha_1$	Mo $K\alpha_1$	Cu $K\alpha_1$
Reflections for cell			
No.	25	25	25
θ range (°)	25–41	10–12	22–42
Intensity measurements			
θ_{max} (°)	75·0	25·0	75·0
ω scan, $(a + b\tan\theta)$, a (°)	0·55	0·75	0·55
ω scan, $(a + b\tan\theta)$, b (°)	0·14	0·35	0·14
Scan speed (° min^{-1})	1·26–10·06	1·18–10·06	1·01–10·06
h	0→10	0→11	0→12
k	0→14	0→20	0→12
l	−27→0	0→29	0→48
Total unique reflections (both sets)	2501 (4688)	3655	2483 (4627)
Reflections with $I \geq 3\sigma(I)$	1691 (3101)	1299	1553 (2879)
% (for a unique set)	67·6	35·5	62·5
Structure refinements			
No. of parameters refined	250	254	350
Data/parameter ratio	6·8	5·1	7·1
Δ/σ mean	0·007	0·001	0·006
maximum	0·095	0·004	0·071
$\Delta\rho$ (e Å^{-3})	−0·70→0·51	−0·15→0·23	−0·32→0·36
R [$I \geq 3\sigma(I)$]	0·069	0·044	0·036
wR	0·082	0·046	0·038
S (goodness of fit)	3·19	1·51	1·39
R (all data)	0·102	0·180	0·077
Extinction, g	5·3(6) × 10^4	12(2) × 10^4	2·6(2) × 10^4

Table 2. *Comparison of observed and calculated values of Δ for the correct absolute configuration of ^{i}Pr/^{i}Pr-a*

h	k	l	Δ_o	Δ_{av}	Δ_c	h	k	l	Δ_o	Δ_{av}	Δ_c
2	1	−20	0·087	0·102	0·040	3	5	−17	−0·366	0·064	0·035
2	8	−2	−0·120	0·006	0·032	2	1	−13	−0·117	0·009	0·030
3	5	−10	0·015	0·024	0·028	3	2	−23	0·375	0·124	0·026
3	3	−3	−0·049	−0·021	0·026	6	4	−17	−0·173	−0·096	0·025
1	4	−12	0·213	0·121	0·024	4	7	−8	0·016	−0·009	0·024
1	3	−9	0·121	0·112	0·023	3	7	−5	−0·129	−0·092	0·022
2	9	−8	0·020	0·061	0·022	1	7	−20	0·031	0·015	0·022
5	5	−8	0·041	0·059	0·022	2	9	−13	−0·035	0·008	−0·021
4	4	−6	−0·104	−0·072	−0·022	5	5	−17	−0·005	−0·012	−0·022
2	6	−9	−0·176	−0·102	−0·023	3	7	−3	−0·103	−0·083	−0·024
2	5	−18	−0·042	0·024	−0·026	4	8	−15	−0·345	−0·136	−0·027
3	1	−9	0·056	−0·062	−0·027	4	6	−4	−0·367	−0·141	−0·027
4	4	−19	0·119	0·094	−0·030	1	11	−10	0·221	0·078	−0·028
5	3	−11	0·530	0·159	−0·034	3	5	−6	0·014	0·029	−0·037
1	4	−1	−0·227	−0·196	−0·037	6	3	−5	−0·076	−0·056	−0·049

Table 3. *Comparison of observed and calculated values of Δ of ^{i}Pr/^{i}Pr-ap for the space group $P4_32_12$ (the correct configuration)*

h	k	l	Δ_o	Δ_{av}	Δ_c	h	k	l	Δ_o	Δ_{av}	Δ_c
6	3	2	0·239	0·100	−0·033	7	5	13	−0·074	−0·161	−0·026
5	1	10	0·273	0·009	−0·021	4	1	5	−0·174	−0·150	−0·023
8	3	3	0·042	−0·169	−0·021	10	2	8	−0·039	−0·061	−0·018
5	4	2	0·059	−0·043	0·017	8	3	4	0·068	−0·098	0·019
8	4	1	0·059	0·012	0·018	9	5	9	−0·014	−0·117	0·018
5	4	9	0·553	0·184	0·019	10	1	6	0·140	0·069	0·020
11	2	3	0·003	0·156	0·018	6	2	5	0·491	0·019	0·021
10	5	10	−0·183	0·029	0·025	5	2	11	0·084	0·074	0·026
6	4	4	0·077	0·052	0·026	5	3	16	−0·095	−0·007	0·028
3	2	14	0·023	0·100	0·027	4	2	4	0·205	0·050	0·031

over two sites and adjusting the split atom occupancies until the isotropic temperature factors of an atom and its split counterpart were approximately the same. The final occupancies that gave the best model are given along with the atomic coordinates. All non-H atoms were allowed to refine anisotropically except the disordered C atoms in ^{i}Pr/^{i}Pr-*a*. H atoms of the two dibenzobarrelenes were placed in calculated positions while the H atoms of the product were refined isotropically after the two sets of data were combined.

Absolute configurations

Before anomalous-dispersion effects were taken into account, the Bijvoet pairs for each chiral structure were included separately in the data sets, taking care not to have duplications for reflections $h = 0$ for ^{i}Pr/^{i}Pr-*a* and $h = k$ for ^{i}Pr/^{i}Pr-*ap*. From the final coordinates obtained from the unique sets of data refinement, the coordinates of the corresponding enantiomorphous molecules for the two compounds were generated (for ^{i}Pr/^{i}Pr-*ap* that meant a change of space group from $P4_12_12$ to $P4_32_12$) and both enantiomorph configurations were refined using the respective combined sets of data for each compound. The final weighted R factors obtained from the refinements are wR [structure (1)] = 0·089886 and wR [structure (2)] = 0·089815 for ^{i}Pr/^{i}Pr-*a*, and wR ($P4_12_12$) = 0·038525 and wR ($P4_32_12$) = 0·038283 for ^{i}Pr/^{i}Pr-*ap*. The quoted wR's for ^{i}Pr/^{i}Pr-*a* are before the disorder was treated. Hamilton's (1965) R-factor ratio test on these values shows that the molecular models in structure (2) and in space group $P4_32_12$ fit the respective observed data better than their opposite models at confidence levels of about 95 and 99%, respectively. However, this test may not be completely reliable (Rogers, 1981), especially given the small values for $\Delta f''$ (0·009 for C, 0·032 for O), and further tests for the absolute configurations employed the Bijvoet difference method (Bijvoet, Peerdeman & Van Bommel, 1951; Hope & de la Camp, 1972; Pennington, Chakraborty, Paul & Curtin, 1988). The differences between the F values of 30 Friedel pairs with the largest Δ_c's were calculated for ^{i}Pr/^{i}Pr-*a*, while 20 pairs were calculated for ^{i}Pr/^{i}Pr-*ap*. Tables 2 and 3 compare the observed and calculated values of $\Delta = (|F^2_{hkl}| - |F^2_{\bar{h}kl}|)/[0{\cdot}5(|F^2_{hkl}| + |F^2_{\bar{h}kl}|)]$ for $h \neq 0$, and $\Delta = (|F^2_{hkl}| - |F^2_{khl}|)/[0{\cdot}5(|F^2_{hkl}| + |F^2_{khl}|)]$ for $h \neq k$ for the correct absolute configurations of ^{i}Pr/^{i}Pr-*a* and ^{i}Pr/^{i}Pr-*ap*, respectively. It is observed from Table 2 that the signs of Δ_o and Δ_c are the same for 19 (out of 30) reflections, and 14 (out of 20) from Table 3. In addition the intensities of the Friedel pairs were remeasured successively at the same scan rate and time. Each Friedel pair was measured six times and the average intensity of each reflection calculated. Δ_{av} in the tables corresponds to the Bijvoet difference of the remeasured and averaged intensities. It is apparent from the tables that the signs for Δ_o and the corresponding Δ_{av} agree except in seven instances for

^{i}Pr/^{i}Pr-*a* and four for ^{i}Pr/^{i}Pr-*ap*. The signs for Δ_{av} and Δ_c are the same for 20 (out of 30) reflections for ^{i}Pr/^{i}Pr-*a* and 14 (out of 20) for ^{i}Pr/^{i}Pr-*ap*, although not necessarily involving the same reflections as those whose Bijvoet difference signs agreed for Δ_o and Δ_c. The lack of complete agreement in the signs of the corresponding Δ's for all the reflections in the tables is not surprising since $\Delta f''$ values are small. In addition the Δ_o, and to some extent the Δ_{av} values, are generally larger than Δ_c; this is not unexpected, since the errors in measurement of Δ_o are much larger than the small anomalous-dispersion differences in Δ_c. All three tests for each structure (Hamilton's test, Bijvoet's test and remeasured Bijvoet data) consistently gave the same results; hence, although the determinations are not completely conclusive, the indications are that the correct absolute configurations have been assigned. Scattering factors were from *International Tables for X-ray Crystallography* (1974). Details of the refinements are in Table 1.

Discussion

Final positional parameters are in Table 4; selected bond lengths and angles involving non-H atoms are in Table 5.* Fig. 2 shows the stereo diagrams of the three molecules with atomic numbering. The geometrical parameters involving the disordered atoms are poorly determined and a relatively large dispersion of individual bond lengths and angles is observed. There are relatively large thermal vibrations in the terminal C atoms of the ester groups of ^{i}Pr/^{i}Pr-*b*, indicative of some disorder; however, no attempts were made to resolve the disorder as no new structural information related to the photochemistry would be provided by splitting the atoms with high anisotropic thermal parameters. Also, the anisotropies of the thermal parameters of the atoms involved in the apparent disorder of ^{i}Pr/^{i}Pr-*b* are relatively smaller than those observed in ^{i}Pr/^{i}Pr-*a* before its disorder was resolved.

Some of the aromatic rings in all three structures show small, but not structurally significant deviations from planarity, χ^2 values being 3·2, 28·2 for ^{i}Pr/^{i}Pr-*a*, 6·3, 25·2 for ^{i}Pr/^{i}Pr-*b*, and 1·15, 19·84 for ^{i}Pr/^{i}Pr-*ap*. The maximum displacements of C atoms from the respective least-squares mean planes of the most non-planar rings are 0·016 (5) Å for ^{i}Pr/^{i}Pr-*a*, and 0·009 (3) Å each for ^{i}Pr/^{i}Pr-*b* and ^{i}Pr/^{i}Pr-*ap*. The dibenzobarrelene ring skeletons in the dimorphs are

* Lists of anisotropic thermal parameters, bond lengths, bond angles and torsion angles, H-atom parameters, and structure factors, and packing diagrams have been deposited with the British Library Document Supply Centre as Supplementary Publication No. SUP 52682 (90 pp.). Copies may be obtained through The Technical Editor, International Union of Crystallography, 5 Abbey Square, Chester CH1 2HU, England.

Table 4. *Final positional (fractional × 10^4) and equivalent isotropic thermal parameters ($U \times 10^3$ Å^2), with estimated standard deviation in parantheses*

$U_{eq} = \frac{1}{3}\sum_i\sum_j U_{ij}a_i^*a_j^*\mathbf{a}_i.\mathbf{a}_j$.

	x	y	z	U_{eq}
^{i}Pr/^{i}Pr-*a*				
C1	7231 (5)	4835 (4)	838 (2)	60
C2	7761 (6)	4136 (5)	362 (2)	65
C3	6715 (6)	3617 (4)	−13 (2)	65
C4	5072 (6)	3721 (4)	73 (2)	54
C4a	4517 (5)	4418 (3)	545 (2)	46
C5	1566 (6)	6563 (5)	325 (2)	73
C6	1611 (8)	7782 (5)	344 (3)	79
C7	2680 (8)	8328 (5)	705 (3)	84
C8	3761 (7)	7696 (4)	1072 (2)	69
C8a	3717 (5)	6530 (4)	1057 (2)	48
C9	4793 (5)	5713 (4)	1413 (2)	46
C9a	5631 (5)	4987 (4)	925 (2)	49
C10	2810 (5)	4667 (4)	719 (2)	45
C10a	2624 (5)	5975 (4)	679 (2)	51
C11	3682 (5)	4904 (4)	1756 (2)	47
C12	2627 (4)	4376 (4)	1399 (2)	45
C13	3934 (5)	4733 (4)	2424 (2)	51
C14	4162 (9)	5661 (5)	3392 (2)	90
C15 (0·7)	2564 (14)	5351 (11)	3727 (5)	122
C15′ (0·3)	3288 (33)	6610 (24)	3696 (12)	112
C16 (0·6)	4545 (20)	6826 (14)	3556 (7)	128
C16′ (0·4)	5708 (26)	6440 (20)	3464 (10)	126
C17	1380 (5)	3555 (4)	1590 (2)	52
C18	−129 (10)	2759 (9)	2427 (3)	118
C19 (0·6)	−1625 (17)	3288 (13)	2461 (6)	103
C19′ (0·4)	−1418 (28)	3774 (21)	2706 (11)	126
C20 (0·7)	461 (16)	2362 (14)	3041 (7)	137
C20′ (0·3)	331 (41)	1910 (32)	2756 (20)	138
O1	3706 (5)	5671 (3)	2737 (1)	84
O2	4388 (6)	3860 (3)	2642 (1)	91
O3	1088 (5)	3593 (4)	2172 (2)	102
O4	698 (5)	2945 (4)	1241 (2)	88
^{i}Pr/^{i}Pr-*b*				
C1	12780 (5)	2136 (3)	6502 (2)	52
C2	13182 (6)	2497 (4)	6973 (3)	63
C3	12266 (7)	2967 (4)	7244 (2)	63
C4	10929 (6)	3082 (3)	7063 (2)	49
C4a	10532 (5)	2712 (3)	6599 (2)	40
C5	8854 (5)	3704 (3)	5538 (2)	52
C6	9256 (7)	3898 (3)	5024 (3)	67
C7	10176 (7)	3439 (4)	4750 (3)	73
C8	10701 (6)	2766 (3)	4984 (2)	57
C8a	10310 (5)	2567 (3)	5492 (2)	43
C9	10822 (5)	1883 (3)	5820 (2)	44
C9a	11449 (5)	2240 (3)	6319 (2)	41
C10	9120 (5)	2753 (3)	6332 (2)	40
C10a	9391 (5)	3037 (3)	5769 (2)	41
C11	9527 (5)	1445 (3)	6011 (2)	43
C12	8662 (5)	1897 (3)	6289 (2)	38
C13	9271 (7)	607 (3)	5889 (2)	52
C14	10366 (7)	−643 (3)	5798 (3)	73
C15	9840 (8)	−1044 (3)	6284 (3)	98
C16	11768 (9)	−891 (4)	5636 (4)	136
C17	7332 (6)	1670 (3)	6537 (2)	41
C18	6168 (7)	748 (4)	7083 (3)	84
C19	5515 (9)	171 (6)	6736 (4)	141
C20	6571 (11)	426 (6)	7608 (4)	172
O1	10455 (4)	206 (2)	5895 (1)	62
O2	8171 (4)	332 (2)	5792 (2)	76
O3	7438 (4)	1037 (2)	6837 (2)	65
O4	6317 (4)	2056 (2)	6493 (2)	66
^{i}Pr/^{i}Pr-*ap*				
C1	6054 (3)	−1627 (3)	6188 (1)	58
C2	6968 (3)	−2628 (3)	6181 (1)	68
C3	7376 (3)	−3155 (3)	5871 (1)	67
C4	6883 (3)	−2705 (3)	5560 (1)	54
C4a	5959 (2)	−1701 (2)	5566 (1)	46
C5	7018 (3)	2227 (3)	5381 (1)	49
C6	7522 (3)	2987 (3)	5648 (1)	60
C7	7063 (3)	2832 (3)	5979 (1)	64
C8	6121 (3)	1910 (3)	6059 (1)	56
C8a	5610 (2)	1160 (2)	5793 (1)	42
C9	4665 (2)	8 (3)	5814 (1)	44
C9a	5545 (2)	−1165 (2)	5881 (1)	46
C10	5251 (2)	−1066 (2)	5276 (1)	44
C10a	6054 (2)	1309 (2)	5455 (1)	40
C11	4219 (2)	−181 (2)	5433 (1)	41

Table 4 (*cont.*)

	x	*y*	*z*	U_{eq}
C12	5320 (2)	429 (2)	5214 (1)	41
C13	2837 (2)	−156 (2)	5317 (1)	43
C14	592 (2)	−179 (3)	5506 (1)	51
C15	151 (4)	−1505 (4)	5380 (1)	77
C16	−74 (3)	207 (4)	5837 (1)	74
C17	−5090 (2)	838 (2)	4845 (1)	43
C18	4608 (3)	2683 (3)	4485 (1)	59
C19	3160 (4)	2749 (5)	4444 (1)	93
C20	5213 (9)	4045 (6)	4492 (2)	150
O1	2005 (1)	−218 (2)	5585 (0·4)	49
O2	2505 (2)	−91 (2)	5019 (0·4)	58
O3	4880 (2)	2117 (2)	4824 (0·4)	51
O4	5113 (2)	101 (2)	4600 (0·4)	59

Table 5. *Selected bond lengths* (Å) *and angles* (°), *with standard deviations in parentheses*

	^{i}Pr/^{i}Pr-*a*	^{i}Pr/^{i}Pr-*b*	^{i}Pr/^{i}Pr-*ap*
C—C (aromatic)	1·34–1·43 (1)	1·372–1·394 (7)	1·374–1·399 (4)
C9—C11	1·521 (6)	1·543 (7)	1·550 (3)
C10—C11	—	—	1·513 (3)
C10—C10a	1·541 (6)	1·517 (6)	—
C10—C12	1·528 (6)	1·533 (6)	1·543 (3)
C10a—C12	—	—	1·494 (3)
C11—C12	1·328 (5)	1·339 (6)	1·537 (3)
C11—C13	1·485 (5)	1·486 (7)	1·479 (3)
C12—C17	1·477 (6)	1·487 (6)	1·503 (3)
C13—O1	1·307 (5)	1·342 (6)	1·340 (3)
C13—O2	1·189 (5)	1·195 (6)	1·200 (3)
C17—O3	1·294 (5)	1·322 (5)	1·323 (3)
C17—O4	1·189 (5)	1·194 (5)	1·207 (3)
C—C—C(aromatic)	118·2–121·8 (5)	118·2–121·7 (6)	118·3–121·5 (3)
C9—C8a—C10a	113·3 (4)	112·7 (5)	109·8 (2)
C9—C9a—C4a	111·6 (3)	112·9 (4)	109·7 (2)
C10—C4a—C9a	112·7 (3)	112·4 (4)	110·0 (2)
C10—C10a—C8a	111·4 (4)	113·2 (5)	—
C12—C10a—C8a	—	—	111·0 (2)
C9—C11—C12	114·0 (3)	113·4 (4)	105·1 (2)
C10—C12—C11	113·5 (3)	113·8 (4)	58·8 (2)

similar to each other and to that of dibenzobarrelene itself (Trotter & Wireko, 1990) and those of other 11,12-diester derivatives (Garcia-Garibay *et al.*, 1990). There are systematic angular deformations from 120° (Allen, 1981*a*) at the benzene–cyclohexene ring junctions (mean angle = 112·5°) which are characteristic of these structures; there are relatively greater angular deformations at the benzene–cyclopentane ring junctions of the dibenzosemibullvalene photoproduct (mean angle = 110·1°), suggesting that such angular distortions are a function of ring size. Bond lengths and angles in the aromatic rings of all three compounds are close to expected values, with mean C—$C_{aromatic}$ = 1·384, 1·385, 1·384 Å, and C—C—$C_{aromatic}$ = 120° each for ^{i}Pr/^{i}Pr-*a*, ^{i}Pr/^{i}Pr-*b*, and ^{i}Pr/^{i}Pr-*ap*, respectively. The lengths of the bridging double bonds (C11=C12) are not significantly different for ^{i}Pr/^{i}Pr-*a* [1·328 (5) Å] and ^{i}Pr/^{i}Pr-*b* [1·339 (6) Å], and are in agreement with the equivalent bridge-bond length of 1·334 (5) Å in the methyl isopropyl diester derivative (Garcia-Garibay *et al.*, 1990), but significantly longer than that in dibenzobarrelene itself [1·316 (4) Å] (Trotter & Wireko, 1990).

The isopropyl ester groups in the starting materials are geometrically inequivalent, especially in the degree of conjugation of the carbonyl groups to the vinyl double bond (C11=C12). The dihedral angles C12—C11—C13—O2 (φ_1) and C11—C12—C17—O4 (φ_2) are 64·1 (7) and −164·3 (5)°, respectively, for ^{i}Pr/^{i}Pr-*a* and 36·1 (9) and −134·1 (6)° for ^{i}Pr/^{i}Pr-*b*. Thus, in both structures, one C=C—C=O system is *syn* and the other *anti*, and the two ester groups are only partially conjugated to the central double bond but to different extents; the carbonyl group at C12 of ^{i}Pr/^{i}Pr-*a* ($\cos^2\varphi_2 = 0{\cdot}93$) is more conjugated to the central vinyl bond C11=C12 than the ester carbonyl group at C11 ($\cos^2\varphi_1 = 0{\cdot}19$).

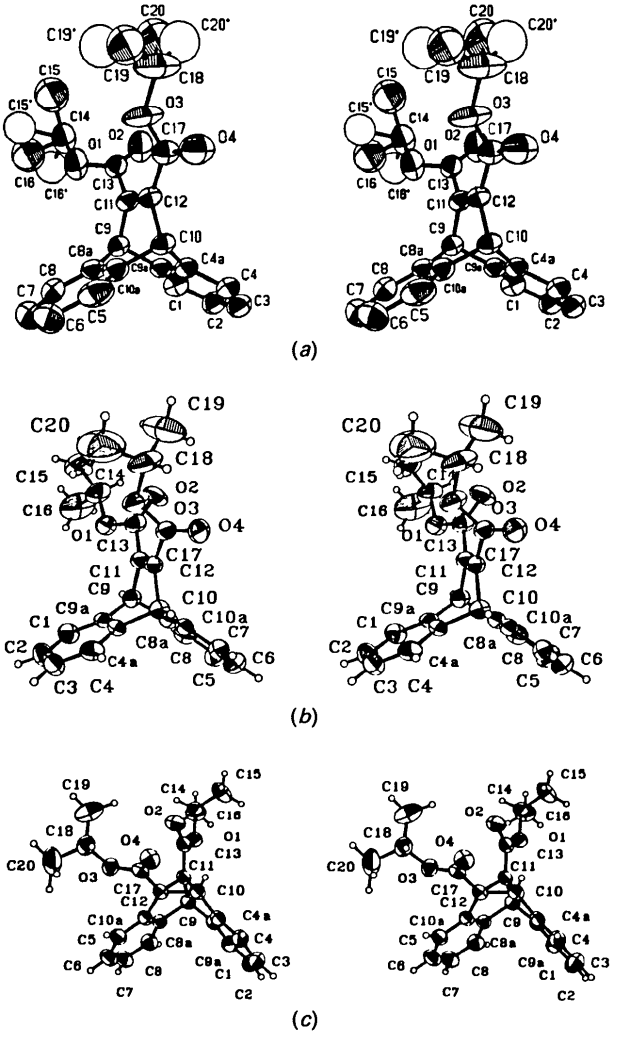

Fig. 2. Stereoviews of the molecular structures (50% thermal probability ellipsoids for the C and O atoms, arbitrary circles for the H atoms). (*a*) ^{i}Pr/^{i}Pr-*a* (disordered C atom with lower occupancies drawn with empty ellipsoids; H atoms omitted for clarity); (*b*) ^{i}Pr/^{i}Pr-*b*; (*c*) ^{i}Pr/^{i}Pr-*ap*. Diagrams (*a*) and (*c*) show the determined absolute configurations for the crystals studied; crystals of ^{i}Pr/^{i}Pr-*b* are racemic, and the enantiomorph shown in (*b*) is numbered to correspond to that shown previously for racemic Me/^{t}Pr [(Garcia-Garibay *et al.*, 1990, Fig. 2(*a*)].

There is an additional strain in the product molecule relative to the starting material as a result of the cyclopentane–cyclopropane ring fusion in the product molecule. Bond angles within the cyclopropane ring are within expected values: 58·8–60·8°. The torsion angles (using the midpoints of the cyclopropane ring bonds, M_{ij} opposite atom C_{ij}, Fig. 3), τ_1 (*M*11—C11—C13—O2) and τ_2 (*M*12—C12—C17—O4) are 10·3 and 46·9° for ^{i}Pr/^{i}Pr-*ap*, respectively. [Note that the ^{i}Pr/^{i}Pr-*ap* numbering system used (Figs. 2 and 3) corresponds to that of the dibenzobarrelene, ^{i}Pr/^{i}Pr-*a*, for comparison purposes, rather than to that of the dibenzopentalene ring system.] Thus, C13=O2 shows a *cis*-bisection conformation with respect to the cyclopropane ring (Allen, 1980, 1981*b*; Garcia-Garibay *et al.*, 1990). No systematic bond-length asymmetry is, however, apparent in the cyclopropane ring. On the other hand, the bond lengths C11—C13 [1·479 (3) Å] and C12—C17 [1·503 (3) Å] seem to suggest some extent of conjugation of C13=O2 to the cyclopropane ring while C17=O4 shows no such effect.

There are some intermolecular contacts in ^{i}Pr/^{i}Pr-*a* below the sum of the van der Waals radii of the atoms involved: O2···H8 (2·58 Å), H3···H16a′ (2·30 Å), H15b′···H19c (2·30 Å), H16c···H19c (2·31 Å), H18···H15c′ (2·32 Å), and H18′···H15c′ (2·36 Å), perhaps an artifact of the disorder. There are no such short intermolecular distances in the other structures.

Structural–photochemical correlations

The commonly accepted mechanism for the di-π-methane reaction (Zimmerman, 1980) can proceed in the dibenzobarrelene system by four pathways, the first steps of which involve bond formation between vinyl (C11 or C12) and benzo C atoms (Fig. 4). For unsymmetrically substituted derivatives (Fig. 4, $E' \neq E$) pathways 1 and 2 lead to two isomeric products, each of which has *S,S,S,S* configuration at the four chiral centres (* in Fig. 4); pathways 3 and 4 give the enantiomeric *R,R,R,R* products. A previous study of the solid-state photolysis of the methyl/isopropyl diester (E/E' = Me/^{i}Pr, Garcia-Garibay *et al.*, 1990) has shown that pathway 2 (and the enantiomeric

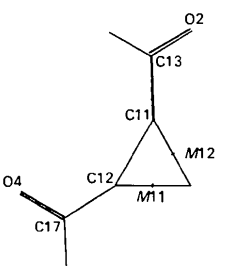

Fig. 3. Geometry of the cyclopropane substructure in ^{i}Pr/^{i}Pr-*ap*.

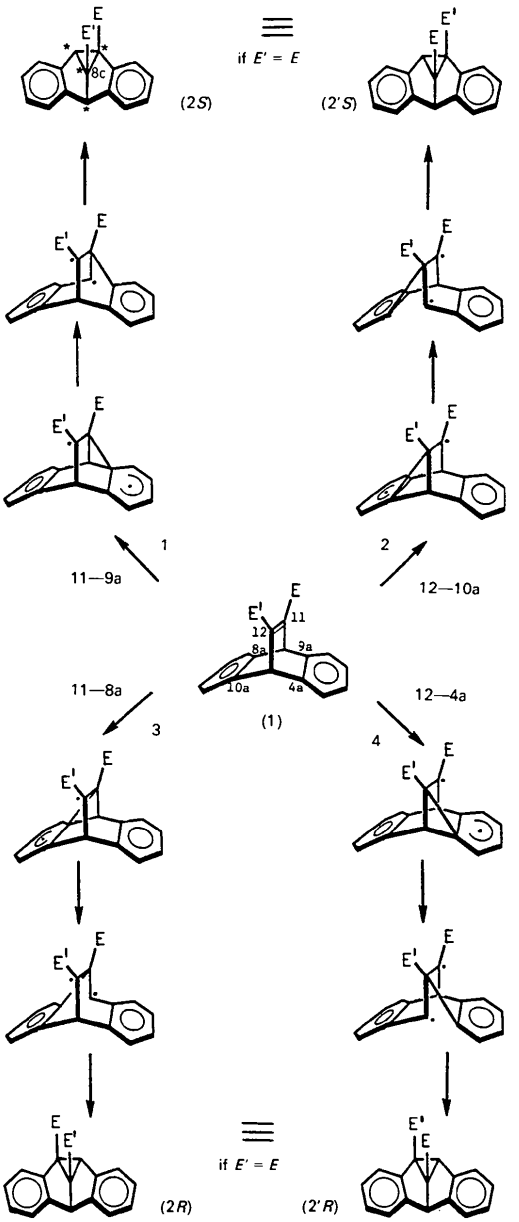

Fig. 4. The four possible pathways in the di-π-methane rearrangement of dibenzobarrelenes. Each path involves three steps, *e.g.* for path 2, (i) C12···C10a bond formation [the C···C distances in the four pathways are all in the range 2·437–2·442 (6) Å], (ii) C10—C10a bond breaking, (iii) C10···C11 bond formation. Each photoproduct contains four chiral centres (* in the drawing at upper left), which are *S,S,S,S* for paths 1 and 2, and *R,R,R,R* for paths 3 and 4. Products (2) and (2′) are isomers, with either *E′* or *E* on the central 8c site (dibenzopentalene numbering system). (The dibenzobarrelene ring system can of course be numbered in four different ways, but all the discussion of the reaction pathways in the text is independent of the numbering system.)

pathway 4, the crystal structure being centrosymmetric) is predominant in the solid state. This pathway is consistent with intermolecular steric effects, as estimated by qualitative inspection of the crystal packing and by more-quantitative calculation of the van der Waals energy as the ester groups move during the solid-state reaction.

For the symmetrically substituted derivative described in the present paper [Fig. 1; (1), $E' = E = CO_2{}^i$Pr), pathways 1 and 2 give rise to identical products [(2) = (2′) in Figs. 1 and 4], and pathways 3 and 4 give the enantiomorphic product. The fortuitous crystallization of one dimorph in the chiral space group $P2_12_12_1$ (^{i}Pr/^{i}Pr-*a*) and the production of chiral photoproduct on solid-state photolysis of this dimorph permit differentiation between pathways (1 + 2) and (3 + 4), by determining the absolute configuration of the molecules of photoproduct. In addition, it may be possible to differentiate between pathways 1 and 2 (or between 3 and 4) by determining the absolute configuration of the $P2_12_12_1$ crystal and correlating this with the absolute configuration of the photoproduct.

The present study of the $P2_12_12_1$ crystal (^{i}Pr/^{i}Pr-*a*) involved growing a large (55 mg) crystal, a small fragment of which was used for the X-ray crystal analysis. The remainder of the large crystal was photolysed and gave laevorotatory photoproduct (^{i}Pr/^{i}Pr-*ap*), $[\alpha]_D = -25{\cdot}4°$ ($CHCl_3$), in quantitative enantiomeric excess. (Presumably multiple crystallizations would give rise to equal amounts of the two chiralities of ^{i}Pr/^{i}Pr-*a*.) The molecular structure of ^{i}Pr/^{i}Pr-*a* can be described by the conformational chirality formalism (Cahn & Ingold, 1951; Cahn, Ingold & Prelog, 1966); basically this designates the conformation of an ester group in ^{i}Pr/^{i}Pr-*a* as *P* (for positive) if the C=C—C=O torsion angle has a positive sign, or as *M* (for minus) for a negative torsion angle. For the crystal of ^{i}Pr/^{i}Pr-*a* studied, the absolute configuration determined [see *Experimental* and Fig. 2(*a*)] is 11*P*, 12*M*, *i.e.* *P* for the ester group at C11 (C12=C11—C13=O2 = +64°) and *M* at C12 (C11=C12—C17=O4 = −164°). The corresponding solid-state photoproduct (^{i}Pr/^{i}Pr-*ap*) crystallizes in space group $P4_32_12$, and the absolute configuration of the molecule has been established (see *Experimental*) as *S*,*S*,*S*,*S* (Fig. 2*c*). Thus the solid-state reaction proceeds *via* pathway 1 (C11—C9a bridging) and/or pathway 2 (C12—C10a bridging), since pathways 3 and 4 would give *R*,*R*,*R*,*R* photoproduct (Fig. 4). A detailed study of the molecular structure of ^{i}Pr/^{i}Pr-*a* indicates that carbonyl O2 is situated above the region of the C4a—C9a bond, and ester O3 above the C11—C12 bond (Fig. 2*a*). Pathways 3 (C11—C8a) and 4 (C12—C4a) involve severe intramolecular clashing of the ester groups as they are forced towards each other in the initial stage of the reaction. In contrast, pathways 1 (C11—C9a) and 2 (C12—C10a) involve movement of the ester groups *away* from one another, thus providing a plausible rationale for the preference for pathways 1 or 2 and the observed *S*,*S*,*S*,*S* photoproduct.

Another point to consider is whether the pathway leading to the observed photoproduct can be deduced on the basis of odd-electron stabilization (Garcia-Garibay *et al.*, 1990), which predicts that initial vinyl–benzo bridging should occur at the vinyl C atom bearing the ester group which is less conjugated to the central double bond (in this case C11, with $\cos^2\varphi_1 = 0{\cdot}19$, *vs* C12, $\cos^2\varphi_2 = 0{\cdot}93$), since this permits more-extensive electron delocalization in the intermediate biradical. This prediction that C11 should be involved in the initial vinyl–benzo bridging is probably not a very reliable indication, since previous work (Garcia-Garibay *et al.*, 1990) has shown that the electron stabilization effects predict the incorrect regioisomer in the unsymmetrical ester case, and are not the major influence in determining the course of the reaction.

The most useful correlation between reactivity and structure was found previously (Garcia-Garibay *et al.*, 1990) by considering intermolecular steric factors. The reaction pathway involves a large movement of a vinyl C atom and its attached ester group, and the most likely reaction pathway will involve movement of the less-sterically hindered ester group. Data on this point can be obtained by three approaches (Garcia-Garibay *et al.*, 1990). Firstly, qualitative inspection of the packing* in the ^{i}Pr/^{i}Pr-*a* crystal structure indicates that the isopropyl ester group at C12 is less sterically hindered than that at C11, so that reaction is expected at C12, *i.e.* pathway 2 (C12—C10a bonding) is the most likely route to the observed *S*,*S*,*S*,*S* photoproduct.

Secondly, a more-quantitative account of the steric effects is obtained from calculation of the 6–12 Lennard–Jones potential-energy profiles (Hagler, Huller & Lifson, 1974), which represent the simulated interaction energy as a result of the movements of the vinyl C atoms and their respective ester groups during initial bond formation (Fig. 5). The angle represents rotation around defined vectors (*e.g.* C10···C11), which moves the appropriate vinyl C atom towards vinyl–benzo bridging: 0° corresponds to the observed molecular structure, and positive and negative angles correspond to clockwise and anticlockwise rotations, respectively [see Garcia-Garibay *et al.* (1990) for further details]. The potential energies were calculated with the coordinates of the molecule before the disorder in the region of the isopropyl groups was treated. Clearly the profiles

* See deposition footnote *re* packing diagram.

suggest that movement of IS19 ($CO_2{}^i$Pr bonded to C12) corresponds to a lower-energy process than movement of IS15 (bonded to C11), and therefore C12 is expected to be involved in the initial bond formation. The expanded profile for IS19 (Fig. 5) shows that if C12 is involved in vinyl–benzo bridging, then anticlockwise rotation about the vector C10···C11 is a less-energetic process than the clockwise rotation. The anticlockwise rotation brings C12 into bond formation with C10a (*i.e.* pathway 2) {see Figs. 2(*a*) and 4; note that Figs. 2(*a*) and 5 of Garcia-Garibay *et al.* (1990) show a molecule of Me/^{i}Pr numbered with the opposite absolute configuration to that determined here for ^{i}Pr/^{i}Pr-*a* [the Me/^{i}Pr crystals are racemic, as are the crystals of ^{i}Pr/^{i}Pr-*b*, and Fig. 2(*a*) of Garcia-Garibay *et al.* (1990) and Fig. 2(*b*) of the present paper depict similar enantiomorphs]}. The ensuing product from such a bond formation is again consistent with the *S*,*S*,*S*,*S* absolute configuration of the observed photoproduct.

Thirdly, pathway 2 is the least-motion (topochemically favorable) process, which produces the photoproduct directly in its observed molecular conformation with only minor rotations of the ester groups (Fig. 6). This is indicated quantitatively in Table 6, which shows calculated torsion angles if the ester groups maintain their starting conformations relative to the C11=C12 bond, and the differences from the observed torsion angles in the photoproduct. Pathway 2 requires changes of 38 and −82° in the two torsion angles, whereas pathway 1 would require much larger reorientations of nearly 180°. (The reaction is not a topotactic one, and the photoproduct was recrystallized prior to the crystal structure analysis. This third argument is therefore not definitive on its own, but is in accord with the previous steric considerations.) Further, the conformational energy values obtained from *MMP*2 calculations (Allinger & Flanagan, 1983) without any minimization show that conformation (2*A*) in Fig. 6 has a conformational energy higher than that of the observed structure by about 23 kcal mol^{-1} (96 kJ mol^{-1}), and so is less likely to be formed.

Thus, the correlation of structural and photochemical data has shown that the odd-electron stabilization concept does not seem to explain adequately the solid-state enantioselectivity of ^{i}Pr/^{i}Pr-*a*. The qualitative inspection of the conformations and the lattice environments of the ester groups, complemented by van der Waals energy calculations and comparison of the conformations of reactant and photoproduct indicate that the enantioselective pathway in the solid state is pathway 2 in Fig. 4.

All of the above discussion of the reaction pathway of the photoconversion of ^{i}Pr/^{i}Pr-*a* to ^{i}Pr/^{i}Pr-*ap* is stated in terms of the atomic numbering system of Figs. 2(*a*) and 4, but is independent of the numbering system. The reaction pathway followed is deduced to be pathway 2, which involves initial bond formation between the vinyl C atom bonded to the more-conjugated ester group and the neighbouring benzo

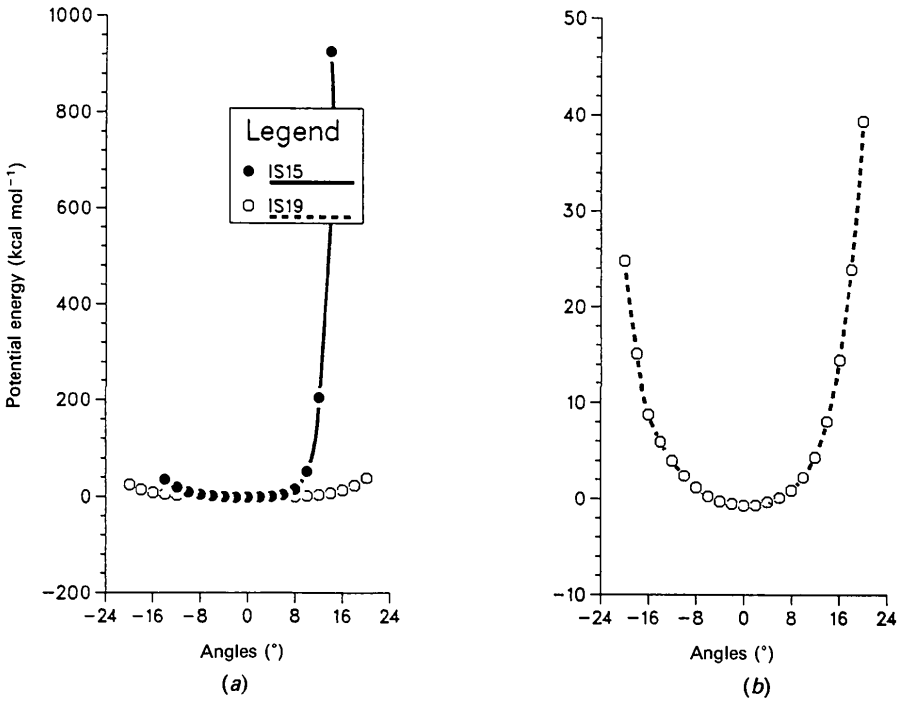

Fig. 5 (*a*) Potential-energy profiles for ^{i}Pr/^{i}Pr-*a*; (*b*) expanded profile of the lower-energy process (movement of IS19). 1 kcal mol^{-1} = 4·1868 kJ mol^{-1}.

C atom which is away from the carbonyl O atom of the less-conjugated ester group, to give the *S,S,S,S* photoproduct.

Finally, the achiral crystal ^{i}Pr/^{i}Pr-*b* (*Pbca*) gives racemic photoproduct on photolysis. The molecular conformation of ^{i}Pr/^{i}Pr-*b* is very similar to that found in ^{i}Pr/^{i}Pr-*a* [Figs. 2(*a*) and 2(*b*)], φ_1 and φ_2 torsion angles of 36 and $-134°$, respectively, for ^{i}Pr/^{i}Pr-*b* (*cf.* 64 and $-164°$ for ^{i}Pr/^{i}Pr-*a*). Thus all of the considerations discussed above for ^{i}Pr/^{i}Pr-*a* probably apply equally to ^{i}Pr/^{i}Pr-*b*, but since we have not studied the crystal structure of the racemic photoproduct, the process will not be discussed in detail. The reaction pathway for the achiral crystals will again involve initial bond formation between the vinyl C atom [C12 in Fig. 2(*b*)] bonded to the ester group with C=O *anti* to C=C, and the neighbouring benzo C atom remote from the carbonyl O atom [O2 in Fig. 2(*b*)] of the *syn* ester group; for the enantiomer and numbering system shown in Fig. 2(*b*) this involves C12—C4a bonding to give finally the *S,S,S,S* photoproduct (the *R,R,R,R* isomer being produced simultaneously from the other enantiomer of ^{i}Pr/^{i}Pr-*b* in the *Pbca* crystal).

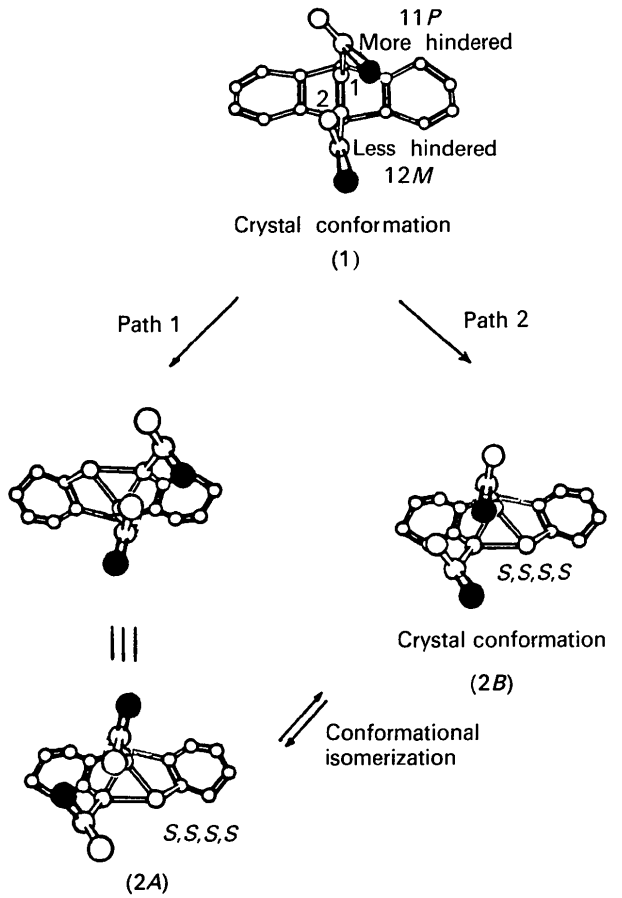

Fig. 6. Conversion of ^{i}Pr/^{i}Pr-*a* (1) to ^{i}Pr/^{i}Pr-*ap* [(2*A*) and (2*B*)]. Pathway 2 involves C12—C10a bonding, and results directly in a conformation close to that observed for the photoproduct, whereas pathway 1 (C11—C9a) would require conformational changes of about 180° in the ester orientations to produce the observed photoproduct conformation. The shaded circles indicate carbonyl O atoms.

Table 6. *Torsion angles* (°) *in the photoreaction of* ^{i}*Pr/*^{i}*Pr-a to give* ^{i}*Pr/*^{i}*Pr-ap*

	C12=C11—C13=O2	C11=C12—C17=O4
^{i}Pr/^{i}Pr-*a*	64	−164
^{i}Pr/^{i}Pr-*ap*		
Calculated for path 1	−164	64
Calculated for path 2	64	−164
Observed	26	−82
(Calc. − obs.) for path 1	170	146
(Calc. − obs.) for path 2	38	−82

We thank the Natural Sciences and Engineering Research Council of Canada for financial support, and the University of British Columbia Computing Centre for assistance.

References

ALLEN, F. H. (1980). *Acta Cryst.* B**36**, 81–96.

ALLEN, F. H. (1981*a*). *Acta Cryst.* B**37**, 900–906.

ALLEN, F. H. (1981*b*). *Acta Cryst.* B**37**, 890–900.

ALLINGER, N. L. & FLANAGAN, H. L. (1983). *J. Comput. Chem.* **4**, 399.

BIJVOET, J. M., PEERDEMAN, A. F. & VAN BOMMEL, J. A. (1951). *Nature (London)* **168**, 271–272.

BUSING, W. R., MARTIN, K. O. & LEVY, H. A. (1962). *ORFLS.* Report ORNL-TM-305. Oak Ridge National Laboratory, Tennesse, USA. Extensively modified by S. J. RETTIG, Univ. of British Columbia, Canada (1976).

BUSING, W. R., MARTIN, K. O. & LEVY, H. A. (1964). *ORFFE.* Report ORNL-TM-306. Oak Ridge National Laboratory, Tennesse, USA.

CAHN, R. S. & INGOLD, C. K. (1951). *J. Chem. Soc.* pp. 612–622.

CAHN, R. S., INGOLD, C. & PRELOG, V. (1966). *Angew. Chem. Int. Ed. Engl.* **5**, 385–415.

EVANS, S. V., GARCIA-GARIBAY, M., OMKARAM, N., SCHEFFER, J. R., TROTTER, J. & WIREKO, F. C. (1986). *J. Am. Chem. Soc.* **108**, 5648–5650.

GARCIA-GARIBAY, M. (1988). PhD Thesis, Univ. of British Columbia, Canada.

GARCIA-GARIBAY, M., SCHEFFER, J. R., TROTTER, J. & WIREKO, F. C. (1990). *Acta Cryst.* B**46**, 79–87.

HAGLER, A. T., HULLER, E. & LIFSON, S. (1974). *J. Am. Chem. Soc.* **96**, 5319–5335.

HAMILTON, W. C. (1965). *Acta Cryst.* **18**, 502–510.

HIXSON, S. S., MARIANO, P. S. & ZIMMERMAN, H. E. (1973). *Chem. Rev.* **73**, 531–551.

HOPE, H. & DE LA CAMP, U. (1972). *Acta Cryst.* A**28**, 201–207.

International Tables for X-ray Crystallography (1974). Vol. IV, pp. 99–102 and 149. Birmingham: Kynoch Press. (Present distributor Kluwer Academic Publishers, Dordrecht).

JOHNSON, C. K. (1976). *ORTEP*II. Report ORNL-5138. Oak Ridge National Laboratory, Tennesse, USA.

MAIN, P., FISKE, S. J., HULL, S. E., LESSINGER, L., GERMAIN, G., DECLERCQ, J.-P. & WOOLFSON, M. M. (1980). *MULTAN*80. *A System of Computer Programs for the Automatic Solution of Crystal Structures from X-ray Diffraction Data.* Univs. of York, England, and Louvain, Belgium.

PENNINGTON, W. T., CHAKRABORTY, S., PAUL, I. C. & CURTIN, D. Y. (1988). *J. Am. Chem. Soc.* **110**, 6498–6504.
ROGERS, D. (1981). *Acta Cryst.* A**37**, 734–741.
SCHEFFER, J. R., TROTTER, J., GARCIA-GARIBAY, M. & WIREKO, F. C. (1988). *Mol. Cryst. Liq. Cryst. Incl. Nonlinear Opt.* **156**, 63–84.
TROTTER, J. & WIREKO, F. C. (1990). *Acta Cryst.* C**46**, 103–106.
ZIMMERMAN, H. E. (1980). *Molecular Rearrangements in Ground and Excited States*, edited by P. DE MAYO, ch. 16. New York: Wiley–Interscience.
ZIMMERMAN, H. E., KECK, G. E. & PFLEDERER, J. L. (1976). *J. Am. Chem. Soc.* **98**, 5574–5581.

Acta Cryst. (1990). B**46**, 440–446

The Use of Single-Wavelength Anomalous Scattering to Solve the Crystal Structure of a Gramicidin A/Caesium Chloride Complex

BY B. A. WALLACE*

Department of Chemistry and Center for Biophysics, Rensselaer Polytechnic Institute, Troy, NY 12180, *USA*

W. A. HENDRICKSON

Howard Hughes Medical Institute, Department of Biochemistry and Molecular Biophysics, Columbia University, New York, New York 10032, *USA, and Laboratory for the Structure of Matter, Naval Research Laboratory, Washington, DC* 20375, *USA*

AND K. RAVIKUMAR

Department of Chemistry and Center for Biophysics, Rensselaer Polytechnic Institute, Troy, NY 12180, *USA*

(*Received* 12 *October* 1989; *accepted* 18 *January* 1990)

Abstract

Single-wavelength Cu $K\alpha$ anomalous scattering has been used to determine the structure of a crystalline complex of gramicidin A and caesium chloride. The asymmetric unit in these crystals, with space group $P2_12_12_1$ and $a = 32{\cdot}118\ (6)$, $b = 52{\cdot}103\ (12)$, $c = 31{\cdot}174\ (7)$ Å, contains four independent monomers (two dimers) of the pentadecapeptide. This structure falls in an intermediate size range for which direct methods and multiple isomorphous replacement are generally not successful for obtaining phase information. However, using the Bijvoet differences and the partial structure of the caesium atoms which have been incorporated in the crystals, it has been possible to obtain information on this crystal form. Because the caesium atoms dominate the scattering of these crystals, inclusion of the Friedel mate information in the restrained least-squares refinement has been essential. These studies extend the utility of single-wavelength anomalous-scattering phase determination to a macromolecular structure in which the partial structure of the anomalous scatterer is large.

Introduction

Gramicidin A is a linear pentadecapolypeptide antibiotic which forms dimeric channels in biological membranes; these channels are specific for the conductance of monovalent cations (Hladky & Haydon, 1972; Veatch & Stryer, 1977). Until recently (Wallace & Ravikumar, 1988; Langs, 1988), no crystal structure of gramicidin had been solved at the molecular level, because the molecule falls in a difficult size range for crystallographic studies: rather large for direct methods, and because of the difficulty in forming isomorphous derivatives of this flexible molecule, somewhat small for multiple isomorphous replacement phasing.

This paper describes the use of anomalous scattering from caesium atoms at a single wavelength (1·54 Å) far removed from the absorption edge of caesium for phase determination in crystals containing a complex of gramicidin and caesium chloride. This type of approach (Hendrickson, Smith & Sheriff, 1985), in which the phases are determined from a combination of the Bijvoet differences and the partial structure of the anomalous scatterer in a single crystal, has been used to solve the structures of a number of macromolecules, including crambin (Hendrickson & Teeter, 1981), myohemerythrin (Smith & Hendrickson, 1982) and trimeric hemerythrin (Smith, Hendrickson & Addison, 1983). In each of these cases, the anomalous scatterer was present in the native protein (the sulfur atoms of the cysteine side chains in crambin, and the iron centers in myohemerythrin and trimeric hemerythrin), and had

* Author to whom correspondence should be addressed.

0108-7681/90/030440-07$03.00